

---

---

RILEM Technical Committee 259-ISR

# Benchmark Problems for AAR FEA Code Validation

---

---

VICTOR SAOUMA<sup>1</sup>  
ALAIN SELLIER<sup>2</sup>  
STÉPHANE MULTON<sup>2</sup>  
YANN LE PAPE<sup>3</sup>  
M-AMIN HARIRI-ARDEBILI<sup>1</sup>

<sup>1</sup> *University of Colorado, Boulder, USA*

<sup>2</sup> *Université de Toulouse, France*

<sup>3</sup> *Oak Ridge National Laboratory, USA*

AUGUST 4, 2017



FOR LATEST VERSIONS.

# Contents

<b>1</b>	<b>Introduction</b>	<b>1</b>
1.1	Objectives	2
1.2	Important Factors in Reactive Concrete	2
1.3	Problems	2
<b>2</b>	<b>Test Problems</b>	<b>5</b>
2.1	P0: Finite Element Model Description	5
2.2	Materials	5
2.2.1	P1: Constitutive Models	5
2.2.1.1	Constitutive Model Calibration	6
2.2.1.2	Prediction	6
2.2.2	P2: Drying and Shrinkage	6
2.2.2.1	Constitutive Model Calibration	7
2.2.2.2	Prediction	8
2.2.3	P3: Basic Creep	8
2.2.3.1	Constitutive Model Calibration	9
2.2.3.2	Prediction	9
2.2.4	P4: AAR Expansion; Temperature Effect	9
2.2.4.1	Constitutive Model Calibration	10
2.2.4.2	Prediction	10
2.2.5	P5: Free AAR Expansion; Effect of RH	11
2.2.5.1	Constitutive Model Calibration	11
2.2.5.2	Prediction	11
2.2.6	P6: AAR Expansion; Effect of Confinement	12
2.2.6.1	Constitutive Model Calibration	12
2.2.6.2	Prediction	12
2.3	Structures	14
2.3.1	P7: Effect of Internal Reinforcement	14
2.3.1.1	Description	14
2.3.1.2	Prediction	14
2.3.2	P8: Reinforced Concrete Beams	14
2.3.2.1	Description	14
2.3.2.2	Prediction	16

---

2.3.3	P9: AAR Expansion; Idealized Dam . . . . .	16
2.3.3.1	Description . . . . .	16
2.3.3.2	Prediction . . . . .	17
2.3.4	P10: Expansion of RC Panel With or Without Lateral Confinement . . . . .	19
2.3.4.1	Description . . . . .	19
2.3.4.2	Predictions . . . . .	25
2.3.5	P11: AAR Expansion of Nuclear Containment Vessel Followed by Earthquake . . . . .	26
2.3.5.1	Description . . . . .	26
2.3.5.2	Prediction . . . . .	27
2.3.5.2.1	Static . . . . .	28
2.3.5.2.2	Dynamic . . . . .	28
<b>3</b>	<b>Results Submission and Workshop</b>	<b>29</b>
3.1	Excel file for Results . . . . .	29
3.2	Workshop . . . . .	29

# List of Figures

2.1	Deterioration of AAR affected concrete (Capra and Sellier, 2003) . . . . .	6
2.2	Drying and Shrinkage test Cases . . . . .	7
2.3	Mass variations for non reactive concrete under various RH conditions; ( <b>multon03</b> ) . . . . .	7
2.4	Strain variations for non reactive concrete under various RH conditions; ( <b>multon03</b> ) . . . . .	8
2.5	Humidity variation . . . . .	8
2.6	Creep in non-reactive concrete under sealed condition for different axial stress; ( <b>multon03</b> ) . . . . .	9
2.7	Stress variation . . . . .	9
2.8	Free expansion from Larive’s tests;( <b>Larive:1998</b> ) . . . . .	10
2.9	Temperature variation . . . . .	10
2.10	Mass variation for reactive concrete under various RH conditions; ( <b>multon03</b> ) . . . . .	11
2.11	Strain variation for reactive concrete under various RH conditions;( <b>multon03</b> ) . . . . .	11
2.12	No vertical stress, no confinement (free swelling);( <b>multon03</b> ) . . . . .	12
2.13	10 MPa vertical stress, no confinement; ( <b>multon03</b> ) . . . . .	13
2.14	Vertical stress of 10 MPa and concrete cast in a 5 mm thick steel container; ( <b>multon03</b> ) . . . . .	13
2.15	Vertical stress of 10 MPa and concrete cast in a 5 mm steel container; ( <b>multon03</b> ) . . . . .	13
2.16	Concrete prism with internal reinforcement . . . . .	14
2.17	Multon’s Beams . . . . .	15
2.18	Mass variation of the beams . . . . .	16
2.19	Idealized dam . . . . .	17
2.20	Yearly variation of pool elevation . . . . .	18
2.21	Specimens . . . . .	20
2.22	Stress Strain curve (28 days) . . . . .	22
2.23	Concrete expansion block tested by Prof. E. Giannini . . . . .	23
2.24	Laboratory measured expansion. Error bars: standard deviation. . . . .	24
2.25	Location of internal concrete gauges . . . . .	24
2.26	Location of deformation sensors . . . . .	26
2.27	Characteristics of the NCVS . . . . .	27
3.1	Sample of Excel based presentation of results . . . . .	30

# List of Tables

1.1	List of Benchmark Problems . . . . .	3
2.1	Characteristics of the three specimens . . . . .	19
2.2	Target mix design . Aggregate quantities are for oven-dry material. Water quantities assume aggregates in saturated-surface dry (SSD) condition. (*) To limit the early-age temperature below $\approx 65^{\circ}\text{C}$ , about 70% of the water was added to the mix as ice cubes. . . . .	21
2.3	Reported 28 days compressive strengths $f'_c$ (MPa) . . . . .	21
2.4	Reported 28 days tensile strengths $f'_t$ (MPa) . . . . .	22
2.5	Reported 28 days elastic modulus $E_c$ (GPa) . . . . .	22
2.6	Provided shrinkage curve data . . . . .	22
2.7	Provided expansion curve data . . . . .	23
2.8	Strain gauges location points. 'S' refers to KM embedded sensors, while 'R' refers to resistive strain gauges placed directly on the rebars. . . . .	25
2.9	Deformation sensor location points . . . . .	25

# 1— Introduction

A number of structures worldwide are known to (or will) suffer from chemically induced expansion of the concrete. This includes not only the traditional alkali aggregate reaction (also known as alkali silica reaction) but increasingly delayed ettringite formation (DEF)<sup>1</sup>.

There are three components to the investigation of structures suffering from such an internal deterioration: a) Chemo-physical characterization focusing primarily on the material; b) Computational modeling of the evolution of damage and assessing the structural response of the structure; and c) managing the structure, (Divet et al., 2003).

Focusing on the second one, ultimately an engineer must make prediction for the response of a structure. In particular: a) is the structure operational, b) is it safe, and c) how those two criteria will evolve in time. This task is best addressed through a numerical simulation (typically finite element analysis) which should account for most of the structure's inherent complexities. This is precisely the object of this document.

The assessment of these finite element codes has been partially assessed within the ICOLD International Benchmark Workshops on Numerical Analysis of Dams<sup>2</sup>, and there were only limited discussion of AAR within the European project *Integrity Assessment of Large Concrete Dams, NW-IALAD*, however there has not yet been any rigorous and rational assessment of codes. Similar recent benchmark analyses of shear walls subjected to reverse cyclic load following AAR expansion, highlighted the need for a more comprehensive benchmark.

Ultimately, practitioners would like to be able to calibrate their model with the limited historical field observation (typically inelastic crest displacements for dams, or crack maps for reinforced concrete) and then use it to extrapolate the behavior of the existing or modified structure into the future. In science and engineering, any extrapolation should be based on a fundamentally sound model which ideally should be independently assessed for its capabilities. Unfortunately, expansive concrete (finite element) models have not yet been assessed within a formal framework. The objective of this effort is indeed an attempt to develop such a formal approach for the benefit of the profession.

Though we are aware of the importance of the chemical constituents of a reactive concrete (part a above), and their potential impact on the residual swelling, this aspect is not considered in this study. Henceforth, we limit ourselves to the interaction of various mechanical aspects: temperature, relative humidity, chemically induced swelling, and mechanical load.

The authors believe that prior to the comparison of analysis of a structures, a series of simple tests should first be undertaken. Each one of the test problems in turn will highlight a strength (or deficiency) of

---

<sup>1</sup>It is well known that DEF is often associated with AAR, however it is increasingly observed that it can occur by itself in massive concrete structure subjected to early age high temperature and under high relative humidity (above 95%).

<sup>2</sup>The sixth (Salzburg) and the eighth (Wuhan) benchmarks invited participants to analyze Pian Telesio and Poggia dams respectively. There was no submission to the former, and only two for the second.

a model, one at a time. Then and only then, we could assess a model predictive capabilities for the analysis of a structure.

This document will describe such a series of tests, and format in which data should be reported. In order to facilitate comparison, the test problems are of increasing complexity. For the most part we assess one parameter at a time, then two, and then three. Only after such an exercise could we compare full blown dam and nuclear containment vessel structure subjected to static and dynamic load.

## 1.1 Objectives

This document is submitted by the authors to the Engineering community for the assessment of finite element codes which can perform a “modern” simulation of reactive concrete expansion.

The study is composed of two parts, the first addresses material modeling, and the second structure modeling. For the material modeling each study is split in two parts: a) parameter identification for the constitutive model (through calibration of your model with provided laboratory test results); and b) Prediction.

## 1.2 Important Factors in Reactive Concrete

Assuming that the final residual swelling of the reactive concrete is known, and based on experimental and field observations, indications are that the following factors<sup>3</sup> should be considered in the finite element analysis of a structure:

1. Environmental Conditions of the concrete
  - (a) Temperature
  - (b) Humidity
2. Constitutive models
  - (a) Solid concrete (tension, compression, creep, shrinkage)
  - (b) Cracks/joints/interfaces.
3. Load history
4. Mechanical Boundary Conditions
  - (a) Structural Arrangement
  - (b) Reinforcement
  - (c) Anchorage

## 1.3 Problems

Table 1.1 describes the 11 problems defined. It should be understood that not all participants will contribute to all of them, but to most of them.

---

<sup>3</sup>There is no general agreement on the importance of all these parameters, the list is intended to be inclusive of all those perceived by researchers to be worth examining.

No.	Description
P0	Textual description of finite element code/models
Material Response	
P1	Constitutive model
P2	Capturing drying and shrinkage
P3	Capturing creep
P4	Effect of Temperature
P5	Effect of RH
P6	Effect of confinement
Structural Response	
P7	Internal reinforcement
P8	Reinforced concrete beam
P9	Dam (simplified)
P10	Reinforced concrete panel expansion
P11	Nuclear containment vessel (Simplified)

Table 1.1: List of Benchmark Problems

This page intentionally left blank.

# 2— Test Problems

## 2.1 P0: Finite Element Model Description

Provide up to five pages of description of the model adopted in this particular order:

### Constitutive Model

1. Basic principles of the model and its implementation.
2. Nonlinear constitutive model of sound or damaged concrete (clarify)
  - (a) Instantaneous response (elasticity, damage, plasticity, fracture and others)
  - (b) Delayed response (creep and shrinkage)
3. Effect on the chemically induced expansion by
  - (a) Moisture
  - (b) Temperature
  - (c) Stress confinement
4. Effect on the mechanical properties of concrete by
  - (a) Expansion
  - (b) Shrinkage and creep

### Finite Element Code Features

1. Gap Element
2. Coupled hydro-thermo-mechanical
3. Others

## 2.2 Materials

In light of the preceding list of factors influencing AAR, the following test problems are proposed. All results are to be entered in the accompanying spreadsheet and formatting instruction strictly complied with (to facilitate model comparison).

### 2.2.1 P1: Constitutive Models

At the heart of each code is the constitutive model of concrete. This problem will assess the code capabilities to capture the nonlinear response in both tension and compression.

It should be noted that in some codes, (Sellier et al., 2009) the constitutive model is tightly coupled (in parallel) with the AAR expansion one (modeled as an internal pressure), in other, (Saouma and Perotti, 2006)

it is more loosely coupled (in series) with the AAR (modeled as an additional strain).

### 2.2.1.1 Constitutive Model Calibration

Perform a finite element analysis of a 16 by 32 cm concrete cylinder with  $f'_c$ ,  $f'_t$  and  $E$  equal to 38.4 MPa, 3.5 MPa and 37.3 GPa respectively<sup>1</sup>. Traction is applied on the top surface, and a frictionless base is assumed. Make and state any appropriate assumption necessary, use the following imposed strain histogram:

$$0 \rightarrow 1.5 \frac{f'_t}{E} \rightarrow 0 \rightarrow 3 \frac{f'_t}{E} \rightarrow 1.5 \varepsilon_c \rightarrow 0 \rightarrow 3 \varepsilon_c \quad (2.1)$$

where  $\varepsilon_c = -0.002$ . If needed, the fracture energy  $G_F$  in tension and compression are equal to 100Nm/m<sup>2</sup> and 10,000 Nm/m<sup>2</sup> respectively.

### 2.2.1.2 Prediction

Units: m, sec., MN, and MPa.

Repeat the previous analysis following an AAR induced expansion of 0.5%, you may use the experimentally obtained degradation curve, by (Institution of Structural Engineers, 1992) and published by Capra and Sellier (2003), Fig. 2.1

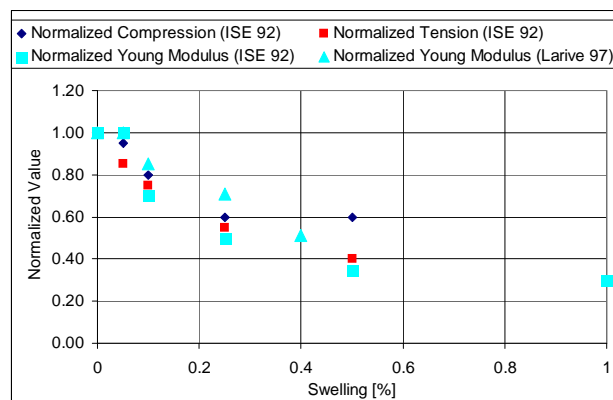


Figure 2.1: Deterioration of AAR affected concrete (Capra and Sellier, 2003)

Results to be tabulated in the accompanying spreadsheet.

## 2.2.2 P2: Drying and Shrinkage

For some structures not necessarily under water (such as bridges or certain hydraulic structures), drying shrinkage strains may be of similar order of magnitude as the AAR induced ones. As shown in Fig. 2.2 one must consider various cases of drying and shrinkage, reactive and non reactive concrete, and at relative humidities ranging from a low 30% to a fully saturated environment, and sealed or not. There are a total of 6 potential cases of interest:

- a. Non reactive concrete at 30% RH
- b. Reactive concrete at 30% humidity

<sup>1</sup>These parameters should be used in all subsequent test problems.

- c. Non Reactive concrete sealed specimen
  - d. Non Reactive concrete under water.
  - e. Reactive Concrete, sealed cylinder.
  - f. Reactive concrete under water.
- which will be analyzed in P2 and P5

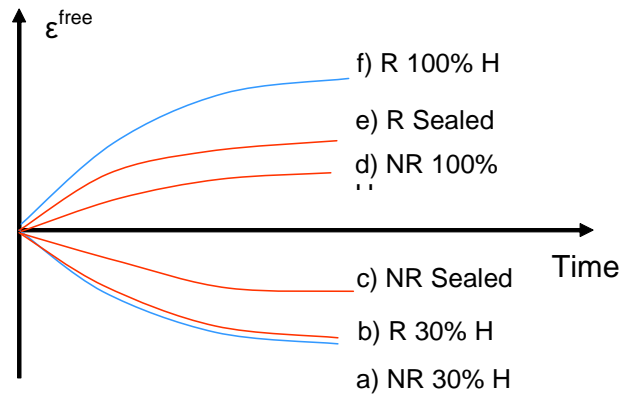


Figure 2.2: Drying and Shrinkage test Cases

### 2.2.2.1 Constitutive Model Calibration

Fit your parameters using a 16 by 32 cm cylinder by performing the following analyses: a, c, and d with respect to the temporal variation of mass (Fig. 2.3) and longitudinal strain (Fig. 2.4)

Mass, Fig. 2.3 and strain, Fig. 2.4 temporal variation<sup>2</sup>.

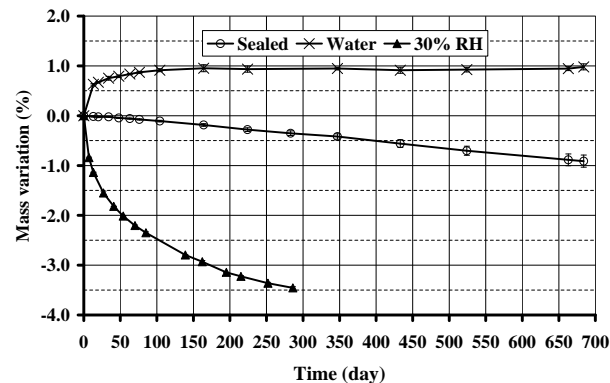


Figure 2.3: Mass variations for non reactive concrete under various RH conditions; (**multon03**)

<sup>2</sup>All available experimental results are tabulated in separate Excel files.

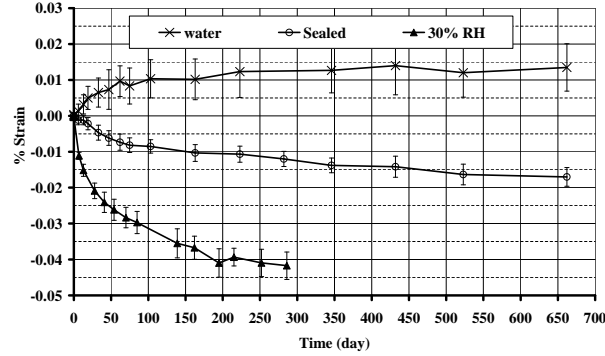


Figure 2.4: Strain variations for non reactive concrete under various RH conditions; (**multon03**)

### 2.2.2.2 Prediction

Units: m, sec., MN, and MPa.

Using the parameter determined from the previous section, repeat the same analysis with the temporal variation of external RH for the cylinder shown in Fig. 2.5.

$$RH(\text{week}) = \frac{RH_{\max} - RH_{\min}}{2} \sin\left(2\pi \frac{t - 16}{52}\right) + \frac{RH_{\max} + RH_{\min}}{2} \quad (2.2)$$

where  $RH_{\max}$  and  $RH_{\min}$  are equal to 95% and 60% respectively.

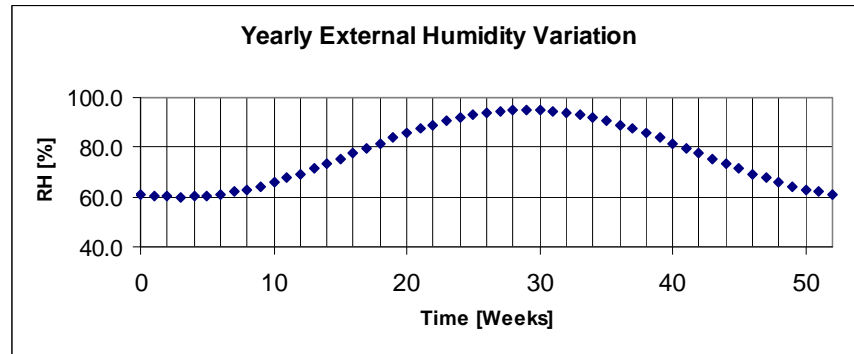


Figure 2.5: Humidity variation

Results to be tabulated in the accompanying spreadsheet.

### 2.2.3 P3: Basic Creep

There is strong experimental and field indications that creep plays a dominant role in the irreversible long term deformation concrete subjected to constant load. Its effect must be accounted for to properly extract the AAR expansion. This may be explained through biaxially or triaxially loaded elements where swelling is restricted in one direction while free to occur on the other(s). Therefore, in the AAR constrained direction creep deformation will be predominant. This is more likely to occur in arch dams.

### 2.2.3.1 Constitutive Model Calibration

For a 13 by 24 cm cylinder subjected to 10 and 20 MPa axial compression, plot the longitudinal and radial displacements. You may calibrate your model on the experimental curve shown in Fig. 2.6.

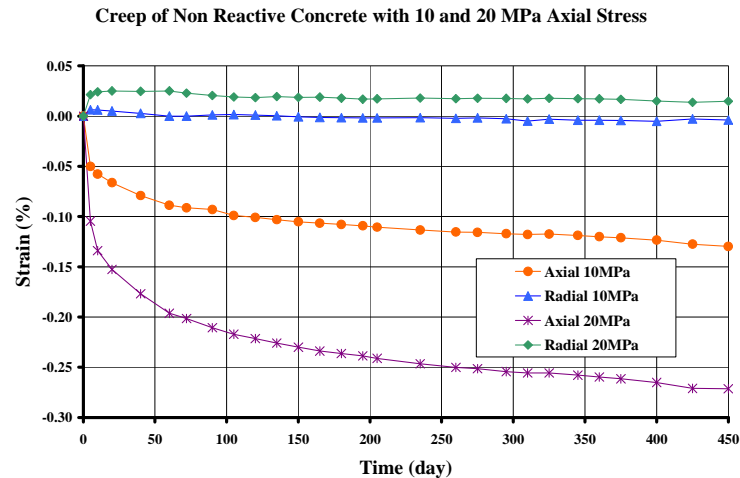


Figure 2.6: Creep in non-reactive concrete under sealed condition for different axial stress; (**multon03**)

### 2.2.3.2 Prediction

Units: m, sec., MN, and MPa.

Using the previously determined parameters, repeat the same analysis for the axial load history shown in Fig. 2.7.

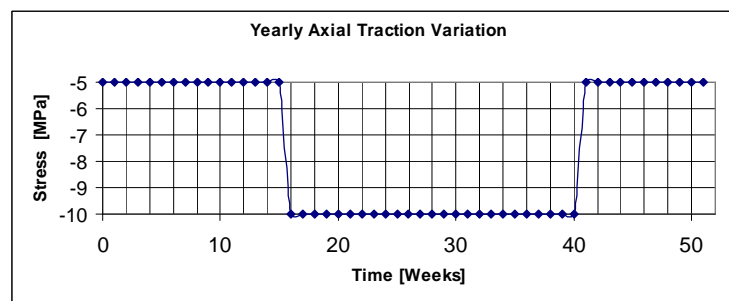


Figure 2.7: Stress variation

Results to be tabulated in the accompanying spreadsheet.

## 2.2.4 P4: AAR Expansion; Temperature Effect

All chemical reactions are thermodynamically driven. Reactive concrete expansion varies widely with temperature ranges usually encountered in the field or laboratories. Hence, it is of paramount importance that the kinetics of the reaction captures this dependency.

### 2.2.4.1 Constitutive Model Calibration

Perform the finite element analysis of a 13 by 24 cm cylinder under water, free to deform at the base and undergoing a free expansion, and for  $T = 23^{\circ}\text{C}$  and  $38^{\circ}\text{C}$ . Fit the appropriate parameters of your model with Fig. 2.8 obtained by Larive:1998

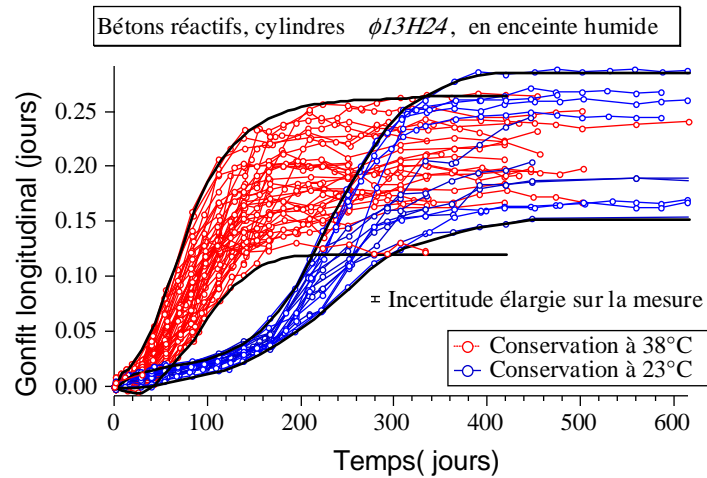


Figure 2.8: Free expansion from Larive's tests;(Larive:1998)

### 2.2.4.2 Prediction

Units: m, sec., MN, and MPa.

Repeat the previous analysis using the variable internal temperature

$$T(\text{week}) = \frac{T_{\max} - T_{\min}}{2} \sin\left(2\pi \frac{t - 16}{52}\right) + \frac{T_{\max} + T_{\min}}{2} \quad (2.3)$$

where  $T_{\max}$  and  $T_{\min}$  are equal to  $25^{\circ}\text{C}$  and  $0^{\circ}\text{C}$  respectively, as shown in Fig. 2.9

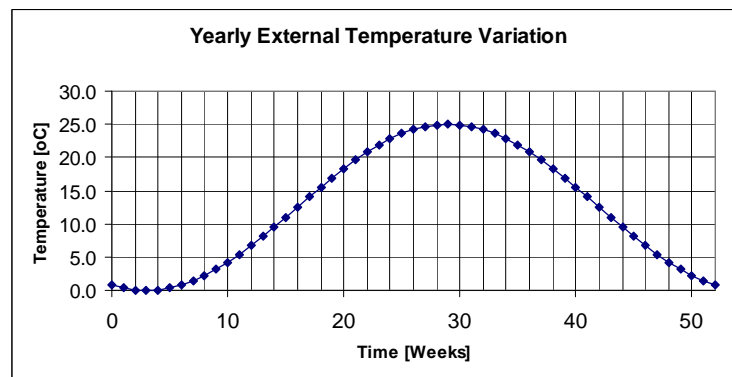


Figure 2.9: Temperature variation

Results to be tabulated in the accompanying spreadsheet.

## 2.2.5 P5: Free AAR Expansion; Effect of RH

Relative humidity plays a critical role in the expansion of AAR affected concrete. It is well established, (Poole, 1992) that expansion will start for a RH at least equal to 80%, and will then increase with RH ( $RH^8$  is a widely accepted formula). For external bridge structures and some dams this can be critical.

### 2.2.5.1 Constitutive Model Calibration

Using a 16 by 32 cm cylinder, and assuming a temperature of 38°C, fit the appropriate parameters for mass and vertical strain variation of reactive concrete as shown in Fig. 2.10 and 2.11 respectively.

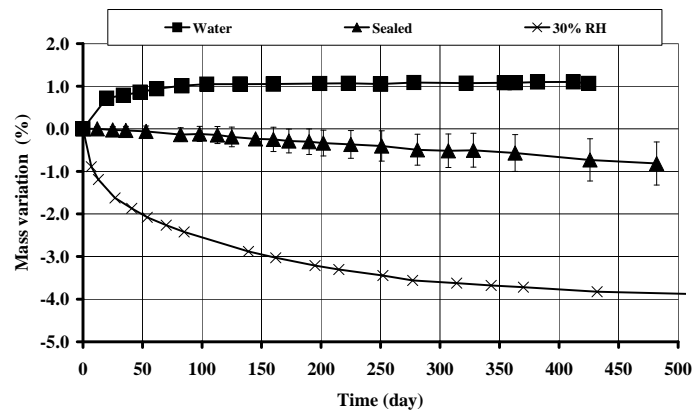


Figure 2.10: Mass variation for reactive concrete under various RH conditions; (**multon03**)

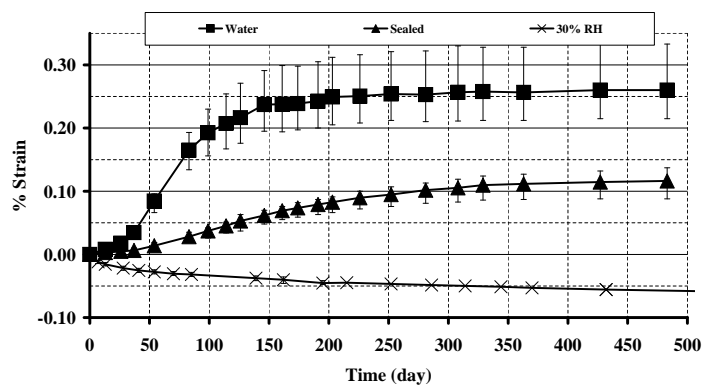


Figure 2.11: Strain variation for reactive concrete under various RH conditions; (**multon03**)

### 2.2.5.2 Prediction

Units: m, sec., MN, and MPa.

Repeat previous analysis using the RH variation shown in Fig. 2.5.

Results to be tabulated in the accompanying spreadsheet.

## 2.2.6 P6: AAR Expansion; Effect of Confinement

It has long been recognized that confinement inhibits reactive concrete expansion, (Charlwood et al., 1992), (Léger, Côte, and Tinawi, 1996) and most recently (Multon and Toutlemonde, 2006). This test series seeks to ensure that this is properly captured by the numerical model.

### 2.2.6.1 Constitutive Model Calibration

For a 13 by 24 cm cylinder, and assuming a temperature of 38°C, analyze the following test cases (all of which consist of sealed specimens):

**P6-a.** No vertical stress, no confinement (Free swelling), Fig. 2.12.

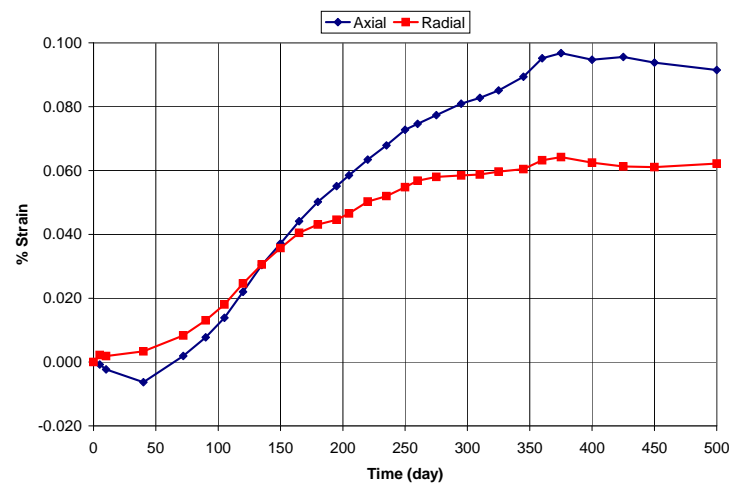


Figure 2.12: No vertical stress, no confinement (free swelling);(multon03)

**P6-b.** Vertical stress of 10 MPa, no confinement, Fig. 2.13.

**P6-c.** No vertical stress, concrete cast in a 5 mm thick steel container, Fig. 2.14.

**P6-d.** Vertical stress of 10 MPa and concrete cast in a 5 mm thick steel container, Fig. 2.15.

In all cases, plot both the axial and radial strains.

### 2.2.6.2 Prediction

Units: m, sec., MN, and MPa.

Repeat the analysis with the vertical and radial imposed stress histogram shown in Fig. 2.7.

Results to be tabulated in the accompanying spreadsheet.

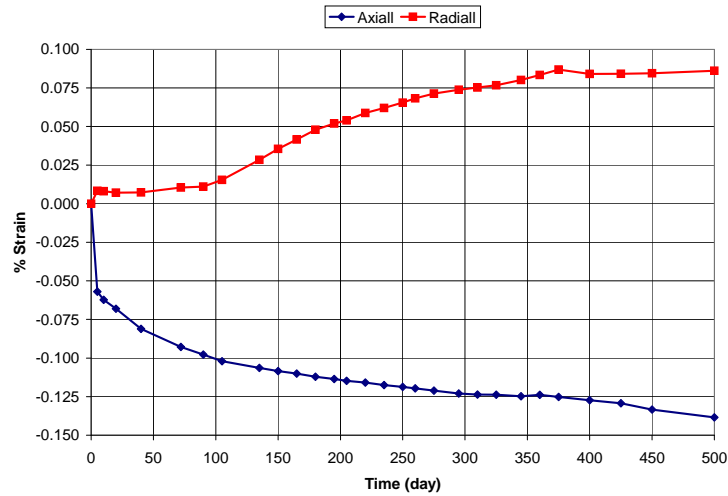


Figure 2.13: 10 MPa vertical stress, no confinement; (**multon03**)

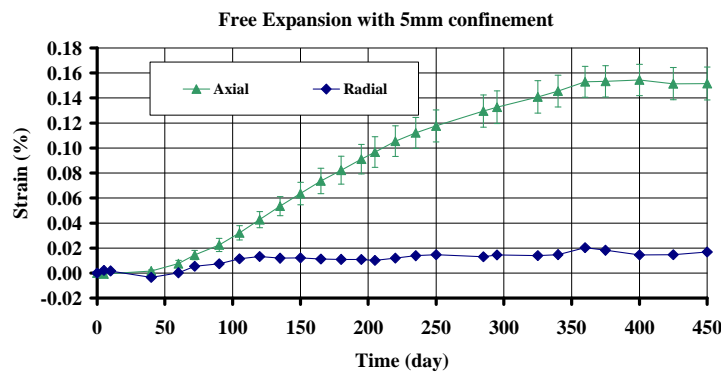


Figure 2.14: Vertical stress of 10 MPa and concrete cast in a 5 mm thick steel container; (**multon03**)

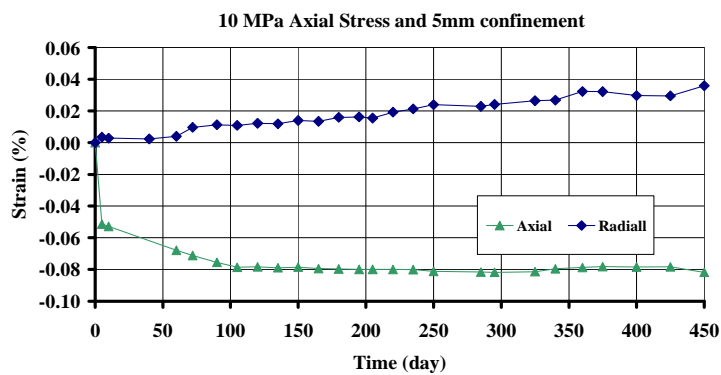


Figure 2.15: Vertical stress of 10 MPa and concrete cast in a 5 mm steel container; (**multon03**)

## 2.3 Structures

### 2.3.1 P7: Effect of Internal Reinforcement

#### 2.3.1.1 Description

Internal reinforcement inhibits expansion and AAR induced cracking would then align themselves with the direction of reinforcement as opposed to the traditional “map cracking”. This test problem seeks to determine how the numerical model accounts for this, especially when cracking (thus a nonlinear analysis is needed) occurs.

Analyze the cylinder of P6-a under the same condition (free expansion, 38°C, 100% RH), for the same duration with a single internal reinforcing bar of diameter 12 mm in the center, and  $E=200,000$  MPa and  $f_y = 500$  MPa.

#### 2.3.1.2 Prediction

Units: m, sec., MN, and MPa.

Determine longitudinal strain in the rebar and the longitudinal and radial strains on the surface of the concrete cylinder. In both cases values are to be determined at mid-height.

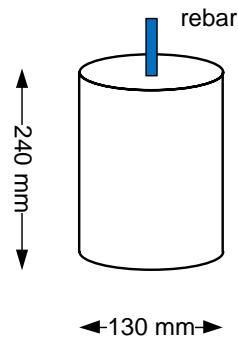


Figure 2.16: Concrete prism with internal reinforcement

Results to be tabulated in the accompanying spreadsheet.

### 2.3.2 P8: Reinforced Concrete Beams

#### 2.3.2.1 Description

The mechanical behavior of two concrete beams, studied by S. Multon during his Ph.D. works at LCPC, is proposed. One beam is damaged by ASR during two years exposure in a 38°C environment and differential water supply, leading to differential ASR expansion within the structures. The other made with non-reactive aggregates was stored in similar conditions. Namely, the effects of the ASR development have been quantified in a 4-points bending test of the beams, resulting in a lot of data among which the residual stiffness and the flexural strength of both reactive and non-reactive beams. The objective is to simulate the evolution of the two beams during the two years of tests, and to finish by a simulation of beam failure in four points bending.

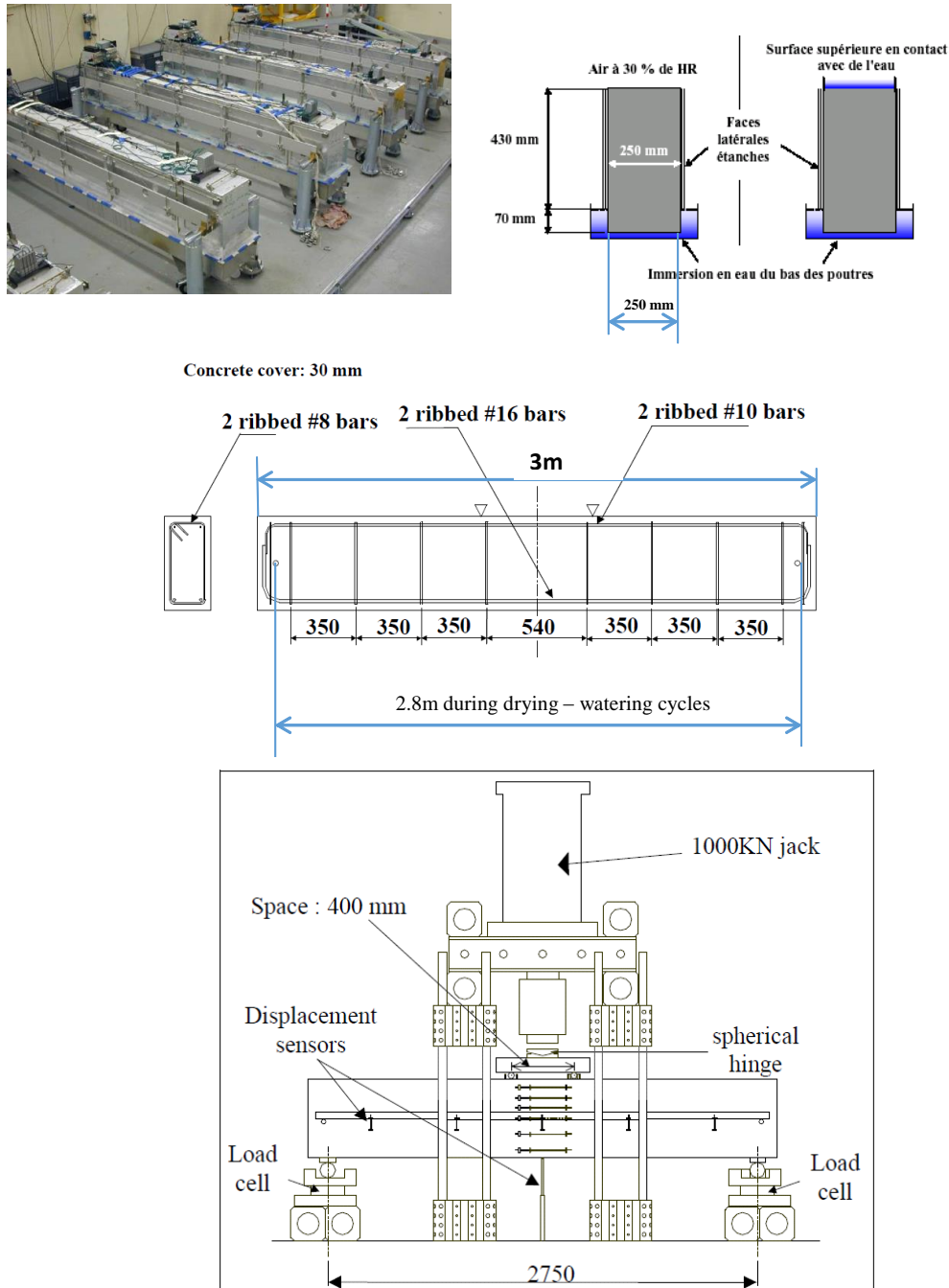


Figure 2.17: Multon's Beams

Material characteristic are the same then in tests P1 to P6, therefore, the LCPC performed tests at several dates since the fabrication (all the results are given in Table 1)

insert table

The whole experimental plan of LCPC involves several beams as mentioned in table 2. In the present benchmark only beams P4 and P6 have to be simulated.

As AAR depends on humidity, a humidity profile must be fitted, in order to consider effect of saturation on the reaction. In order to fit the drying-humidification cycle, the mass evolutions of the beams are given below

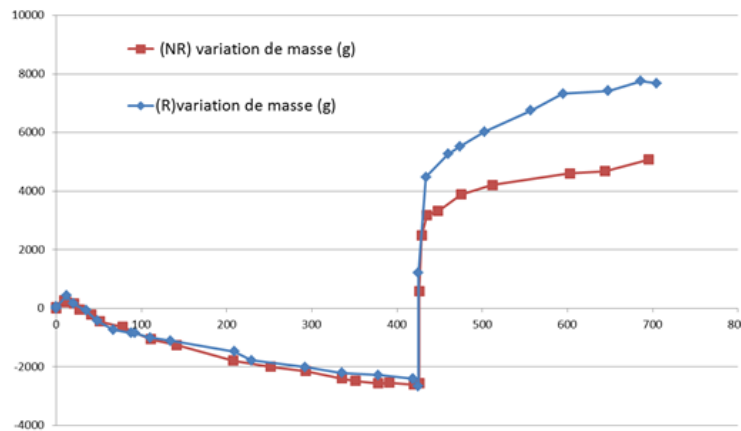


Figure 2.18: Mass variation of the beams

The temperature is constant and equal to 38°C. The concrete porosity is around 16% (15% at the bottom and 17% at the top of the beam).

### 2.3.2.2 Prediction

Units: m, sec., MN, and MPa.

- The first objective is to find a realistic humidity profile compatible with the mass variation history given in figure 2.17.
- The second objective is to predict the deflection of each beam, at mid span, versus time
- The third objective is the evolution of stress versus time, in the bottom longitudinal reinforcement #16, at mid span.
- The last stage consists to simulate, for the two beams, a four point bending test schematized in Fig. 2.18. Participants have to provide the Force-deflection curve until failure of each beam.

Results to be tabulated in the accompanying spreadsheet.

## 2.3.3 P9: AAR Expansion; Idealized Dam

### 2.3.3.1 Description

This last test problem assesses the various coupling amongst various parameters as well as the finite element code and its ability to simulate closure of joint. A common remedy for AAR induced damage in dams is to cut a slot in the structure as in Mactaquac (Gilks and Curtis, 2003). This will relieve the state of stress, and allow the concrete to expand freely. However, at some point concrete swelling will result in a contact between the two sides of the slot. Hence, this problem will test the model ability to capture this important simulation aspect as well.

Consider the reduced dam model shown in Fig. 2.19 with the following conditions: a) lateral and bottom faces are all fully restrained; b) front back and top faces are free; c) slot cut at time zero, total thickness 10

cm; d) concrete on the right is reactive, and concrete block on the left is not reactive; e) hydrostatic pressure is applied only on the right block.

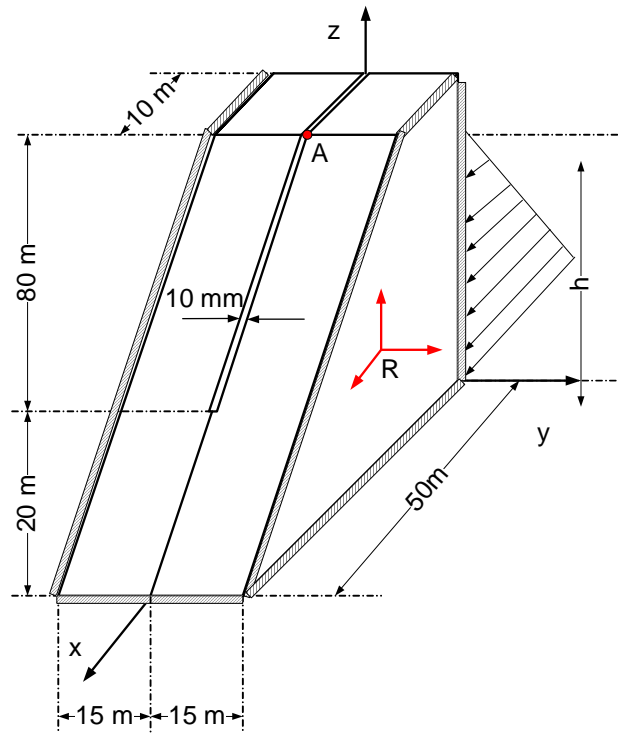


Figure 2.19: Idealized dam

### 2.3.3.2 Prediction

Units: m, sec., MN, and MPa.

Using the fitting data of P6, and an friction angle of  $50^{\circ}C$  for concrete against concrete, and zero cohesion, consider two cases:

- Homogeneous field of internal temperature ( $20^{\circ}C$ ), relative humidity (100%), and an empty reservoir.
- Transient field of external temperature Fig. 2.9, relative external humidity Fig. 2.5, and pool elevation variation Fig. 2.20 given by where  $EL_{max}$  and  $EL_{min}$  are equal to 95 and 60 respectively.

For both analysis, the specified temperature and relative humidity is the one of the concrete surface. Zero flux condition between dam and foundation. Reference base temperature of the dam is  $20^{\circ}C$ .

- $x$ ,  $y$ ,  $z$  displacements of point A.
- $F_x$ ,  $F_y$  and  $F_z$  resultant forces on the fixed lateral face versus time (25 years). Assume the typical yearly variations of external air temperature and pool elevation shown in Fig. 2.9 and 2.20 respectively.

This model seeks to capture: a) general finite element program capabilities in modeling the joint response; b) ease (or difficulty) in preparing the input data file for a realistic problem; and c) coupling of the various parameters.

$$EL(\text{week}) = \frac{EL_{max} - EL_{min}}{2} \sin\left(2\pi \frac{t}{52}\right) + \frac{EL_{max} + EL_{min}}{2} \quad (2.4)$$

where  $EL_{max}$  and  $EL_{min}$  are equal to 95 and 60 respectively.

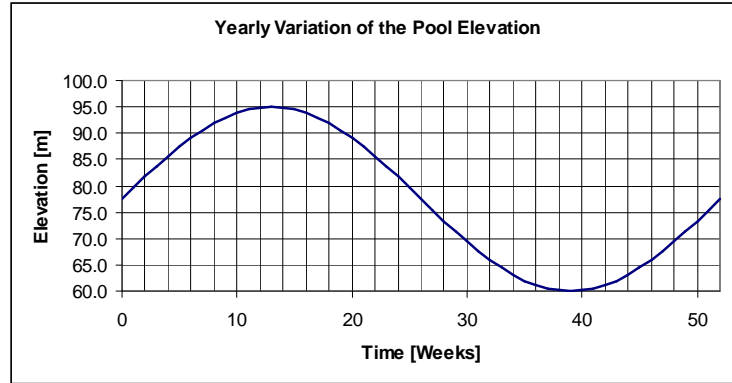


Figure 2.20: Yearly variation of pool elevation

Results to be tabulated in the accompanying spreadsheet.

### 2.3.4 P10: Expansion of RC Panel With or Without Lateral Confinement

This section has been prepared with the assistance of Nolan Hayes, Ammar Abd-Elssamd and Qiang Gui from the University of Tennessee, Knoxville.

The University of Tennessee, Knoxville (UTK), under U.S. Department of Energy (DOE) subcontract managed by Oak Ridge National Laboratory (ORNL), have been performing large scale laboratory testing of confined and unconfined concrete blocks (simulating a typical reinforced concrete member found in light water reactor nuclear power plants).

The objective of this benchmark test case is to perform predictive numerical simulations of two large-scale reinforced concrete blocks (with different boundary conditions) and compare the simulation results with the already collected monitoring data.

#### 2.3.4.1 Description

**Geometry** The laterally-confined reinforced concrete reactive specimen, referred to as *CASR* ('C' for confined), is cast inside a rigid steel frame while a similar reinforced concrete reactive specimen, referred to as *UASR* ('U', for unconfined) is allowed to expand without lateral restraints. A third specimen, non-reactive, referred to as *CTRL*, for control, is also not subjected to lateral restraints. See summary in Table 2.1

All three specimens of dimensions,  $136'' \times 116'' \times 40''$  (length, width and height; x-y-z axis), i.e.,  $3.453 \text{ m} \times 2.946 \times 1.016 \text{ m}$ , Fig. 2.21 are reinforced near the top and the bottom faces by two welded layers of orthogonal rebars: (22) #11 bars (1.41" nominal diameter, cross section area:  $1006 \text{ mm}^2$ ), (10) in one direction and (12) in the perpendicular direction, placed in horizontal planes – See Fig. 2.21(d) for layout. Rebars are made of standard carbon steel. Square plate heads ( $4'' \times 4'' \times 1''$ , i.e.,  $10.16 \text{ cm} \times 10.16 \text{ cm} \times 2.54 \text{ cm}$ ) are welded to the rebar extremities. The concrete cover, in the least distance to the concrete outer surface, is 3" (7.62 cm). There is no reinforcement in the third, i.e., vertical, direction, to the exception of (6) #11 debonded rebar spacers placed inside of pipes to allow free vertical expansion during the test.

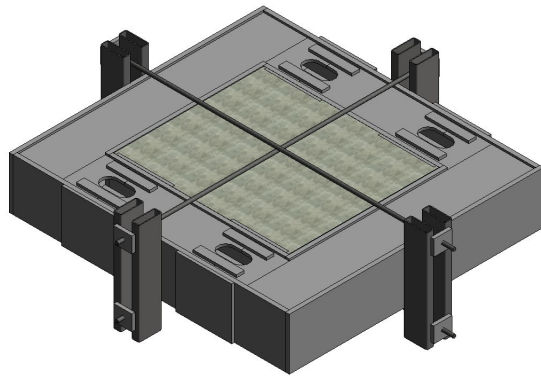
**Steel Confinement Frame** The steel plate girder frame was designed with the primary goal of maximizing stiffness in bending. In order to achieve this goal, 3" thick plates, height 3'4", were chosen as flanges to the plate girder. These flanges are connected by three 2" thick web plates, length 2'10". All steel was manufactured from A572 Grade 50 steel plate. Design of splice plate connection not provided here is available upon request.

In order to reduce frictional effects between the steel frame and the concrete specimen, a single layer (thickness: 1.5 mm) of high-density polyethylene (HDPE) was introduced at the interface, providing a low steel-HDPE friction coefficient estimated by the vendor around 0.3 and unilateral contact conditions.

**Additional Post-tensioned system** Four threadbar post-tension bars (2 in each direction, 2.5 inches dia.)

Table 2.1: Characteristics of the three specimens

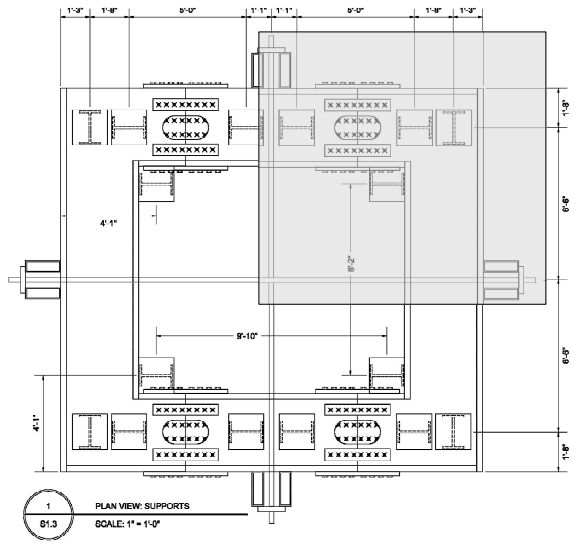
ID	Label	Confined	Reactive
1	CASR	Yes	Yes
2	UASR	No	Yes
3	CTRL	No	No



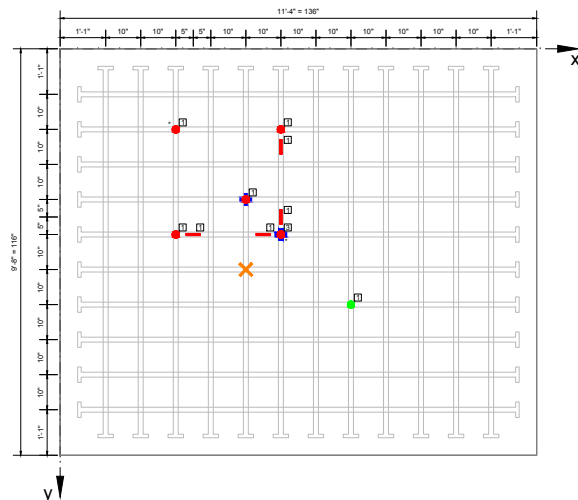
(a) Computer rendering of the confined specimen (CASR)



(b) Form construction in UTK Civ. Env. Eng. high bay



(c) Confined specimen layout – Top view. (Shaded area indicating symmetries)



(d) Reinforcement layout – Top view. Bottom and top reinforcement layout are identical.

Figure 2.21: Specimens

manufactured by DYWIDAG-Systems International (DSI) were installed in [September 2016](#), in order to increase the confining force, if necessary. It is initially just slightly tightened to avoid “slack”, and has remained, as of today.

**Casting and Curing** Casting took place July 23rd 2016. In an attempt to mitigate potential crack sources other than ASR, the formworks were insulated by placing rigid foam sheathing insulation with an R-value of three around the side and on top of the specimens, shortly after pouring. The insulation was placed with edges overlapping and secured in place with tape and plastic wrap.

All formworks were removed on August 4, 2016. Each large specimen and concrete cylinder, for further materials testing, was covered with wet burlap to prevent moisture loss. The burlap was periodically moistened as required to keep the concrete surfaces wet.

A few days after casting, the bottom support is removed, and the concrete block is vertically supported

by four 18" × 18" (45.7 cm × 45.7 cm) corner plates. Plates are directly supporting the specimens on the concrete surface. The estimated steel-concrete friction coefficient is ≈0.6.

**Operation** A modular environmental chamber was designed by Norlake Scientific with the initial primary goals for temperature and humidity control being 100°F ± 2°F (38°C ± 1°C) and 95% ± 5%. The chamber was initialized for full operation early morning August 19, 2016.

The chamber is periodically shutdown for inspection on a average frequency of 2 days per month. During shutdowns, the average temperature and RH are about ≈77°F (25°C) and 60% (transient of about 4 hours). After the shutdown period, the chamber is restarted and the temperature and humidity return to the original set points within 6 hours.

**Target mix design** The mix design has been extensively investigated at the University of Alabama, and the one retained, including a reactive and a control mix, is shown in Table 2.2 with 1" (25 mm) maximum size aggregate (MSA) composed of Green schist – muscovite, chlorite, quartz, Na-feldspar, K-feldspar, calcite, and, cristobalite.

In this mix, only the coarse aggregate is reactive. A 50% sodium hydroxide solution (NaOH) is used to increase the alkali loading of the reactive mix to 5.25 kg.m<sup>-3</sup>, and a 30% lithium nitrate solution (LiNO<sub>3</sub>) is used at 150% of the manufacturer's recommended dosage to mitigate ASR for the control mix.

Table 2.2: Target mix design . Aggregate quantities are for oven-dry material. Water quantities assume aggregates in saturated-surface dry (SSD) condition. (\*) To limit the early-age temperature below ≈ 65°C, about 70% of the water was added to the mix as ice cubes.

Materials	Quantity, kg.m <sup>-3</sup> (lb.yd <sup>-3</sup> )	
	Reactive	Control
Coarse Aggregate	1180 (1988.8)	1180 (1988.8)
Fine Aggregate	728 (1226.6)	728 (1226.6)
Cement	350 (590)	350 (590)
Water(*)	175 (295)	175 (295)
w/c	0.5	0.5
NaOH solution	9.8 (16.6)	-
LiNO <sub>3</sub> solution	-	11.9 (20.03)

**Mechanical properties** 28 days mechanical properties compressive and tensile strengths, and the elastic modulus are shown in Table 2.3, 2.4 and 2.5, respectively along with their mean and standard deviations.

Table 2.3: Reported 28 days compressive strengths  $f'_c$  (MPa)

Specimen Type	AVG	STD
CASR	22.2	2.07
UASR	20.7	1.17

CASR: Confined Reactive Specimen

UASR: Unconfined Reactive Specimen

A representative 28 days stress-strain curve is shown in Fig. 2.22.

**Shrinkage** Shrinkage has been measured in the CTRL specimen. The datapoints for the shrinkage curve are shown in Table 2.6.

info to be added.

**Expansion curves obtained from earlier material testing** Expansion curves were obtained by Pr. E.

Table 2.4: Reported 28 days tensile strengths  $f'_t$  (MPa)

Specimen Type	AVG	STD
CASR	2.70	0.215
UASR	2.13	0.044

CASR: Confined Reactive Specimen

UASR: Unconfined Reactive Specimen

Table 2.5: Reported 28 days elastic modulus  $E_c$  (GPa)

Specimen Type	AVG	STD
CASR	34.5	3.03
UASR	34.4	2.22

CASR: Confined Reactive Specimen

UASR: Unconfined Reactive Specimen

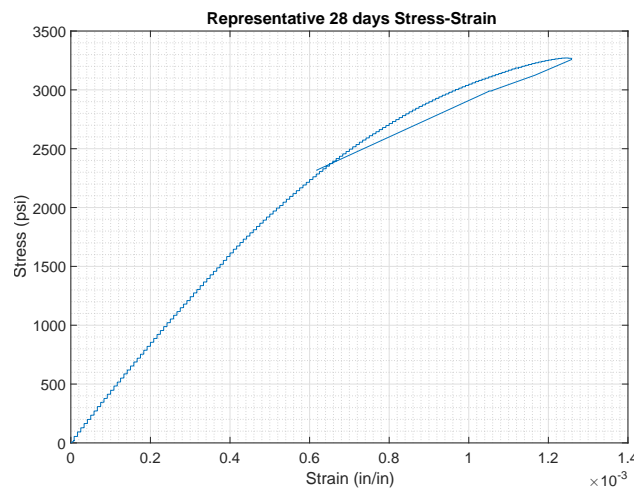


Figure 2.22: Stress Strain curve (28 days)

Table 2.6: Provided shrinkage curve data

<b>Measured Shrinkage</b>	
Age (Days)	Shrinkage
5	-0.0031%
10	-0.0104%
20	0.0162%
30	-0.0178%
40	-0.0185%
50	-0.0190%
60	-0.0194%
100	-0.0214%
200	-0.0245%
300	-0.0275%

Giannini, at the University of Alabama (UA), while testing different aggregates-forming concrete. The concrete blocks,  $300 \times 300 \times 600$  mm, are stored in UA climate chamber at  $38^\circ\text{C}$  and 95%RH, shown in Fig. 2.23, and their expansion was periodically monitored using DEMEC points.

Data are tabulated in Table 2.7 and shown in Fig. 2.24 where the vertical expansions were taken over



Figure 2.23: Concrete expansion block tested by Prof. E. Giannini

a 150 mm gauge length, and longitudinal expansions (same direction as longitudinal) were taken over a 500 mm gauge length. It should be noted that the reported mean (or average) corresponds to the average of all the experimental values.

Table 2.7: Provided expansion curve data

Calculated Expansions		
Age (Days)	Average Exp.	STD
6	0.000%	0.0000%
40	-0.004%	0.0045%
68	0.000%	0.0031%
87	0.012%	0.0081%
103	0.020%	0.0091%
117	0.028%	0.0103%
138	0.045%	0.0193%
152	0.057%	0.0250%
170	0.070%	0.0307%
190	0.088%	0.0382%
220	0.103%	0.0440%
304	0.146%	0.0634%
312	0.157%	0.0733%
350	0.165%	0.0729%
371	0.174%	0.0782%
459	0.192%	0.0885%
504	0.197%	0.0903%

**Recorders/sensors location** Recorder<sup>3</sup> locations are shown as follows:

**Embedded KM strain transducer (KM-100B)** , referred as *strain gauges*, gauge length 100 mm, in Fig. 2.25 and Table 2.8.

<sup>3</sup>In a finite element analysis, point from which we determine computed values are commonly referred to as “recorders”

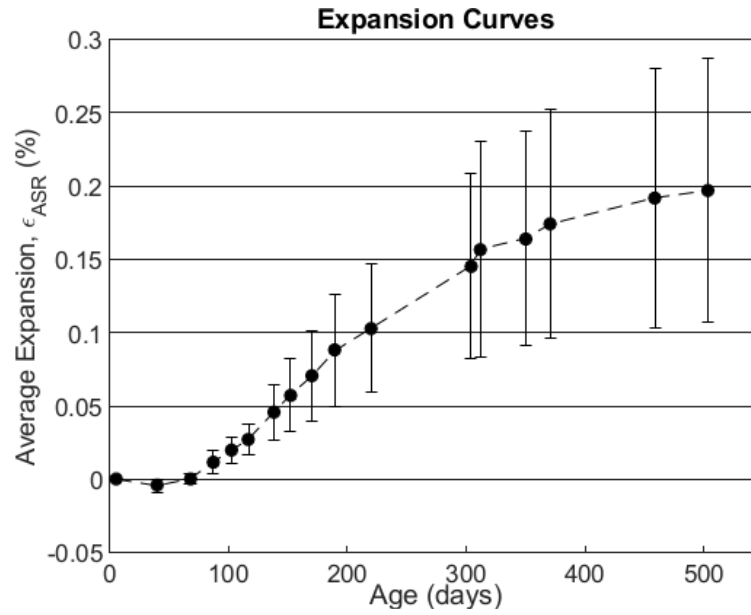


Figure 2.24: Laboratory measured expansion. Error bars: standard deviation.

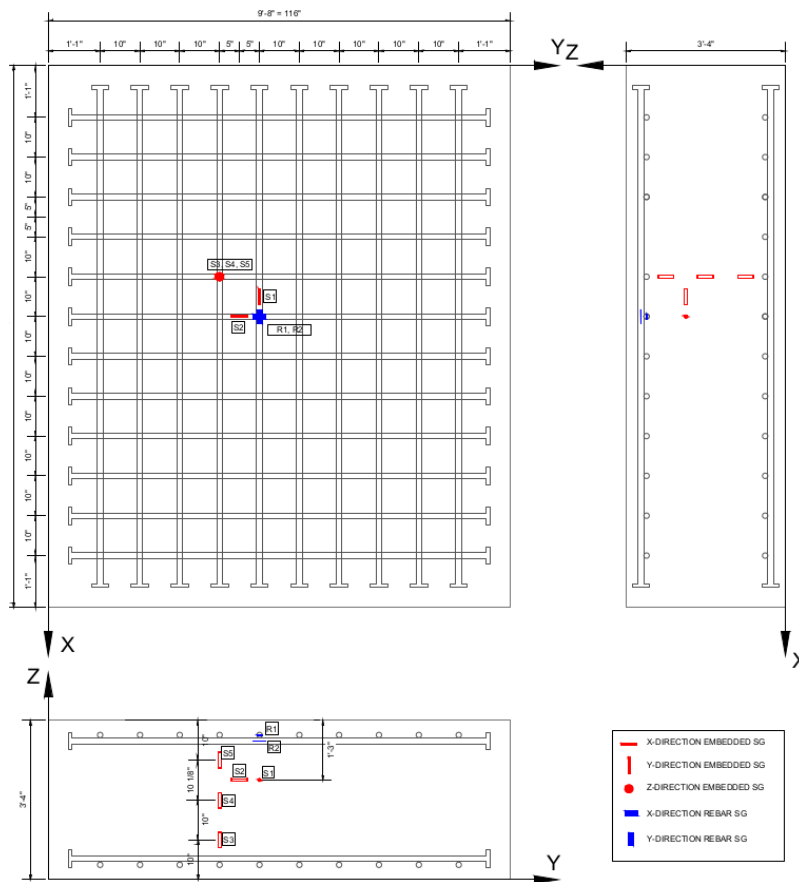


Figure 2.25: Location of internal concrete gauges

Continued on next page

		Coord. [inches]			Coord. [meter]		
id	dof	x	y	z	x	y	z

Table 2.8: Strain gauges location points. 'S' refers to KM embedded sensors, while 'R' refers to resistive strain gauges placed directly on the rebars.

		Coord. [inches]			Coord. [meter]		
ID	DOF	x	y	z	x	y	z
S1	1	58	53	25	1.473	1.346	0.635
S2	2	63	48	25	1.600	1.219	0.635
S3	3	53	43	10	1.346	1.092	0.254
S4	3	53	43	20	1.346	1.092	0.508
S5	3	53	43	30	1.346	1.092	0.762
R1	1	63	53	36.375	1.600	1.346	0.924
R2	2	63	53	34.875	1.600	1.346	0.886

**Resistive strain gauges** General purpose resistive strain gauges (gauge length: 1.52 mm) were attached to the reinforcing bars in the specimens. These sensors are attached to the top and bottom of the rebar in the select locations to measure rebar strain. The location of resistive strain gauges of interest are shown in Fig. 2.25 and Table 2.8.

**Long gauges fiber-optics-based deformation sensors** (SOFO, gauge length  $\approx$  1.0–1.5 m with location) measure (1) the vertical deformation between the bottom and top rebars layers, and, (2) horizontal deformation at the bottom surface as illustrated and tabulated in Fig. 2.26 and Table 2.9

Table 2.9: Deformation sensor location points

		Start Coord. [inches]			End Coord. [inches]			Start Coord. [meter]			End Coord. [meter]		
ID	DOF	x	y	z	x	y	z	x	y	z	x	y	z
D1	3	91	45	4.25	91	45	35.75	2.311	1.143	0.108	2.311	1.143	0.908
D2	3	45	71	4.25	45	71	35.75	2.311	1.143	0.108	2.311	1.143	0.908
D3	1	45	26	0	104	26	0	1.143	0.660	0	2.642	0.660	0
D4	1-2	38.75	28.75	0	89.75	79.75	0	0.984	0.730	0	2.280	2.026	0

**Test duration** Casting occurred July 23rd 2016. Assuming testing will end April 19, 2019, it is requested to model a total duration of 1,000-days.

#### 2.3.4.2 Predictions

Units: m, sec., MN, and MPa.

Plot for both specimens, CASR and UASR, as a function of time (increments of one month) the following

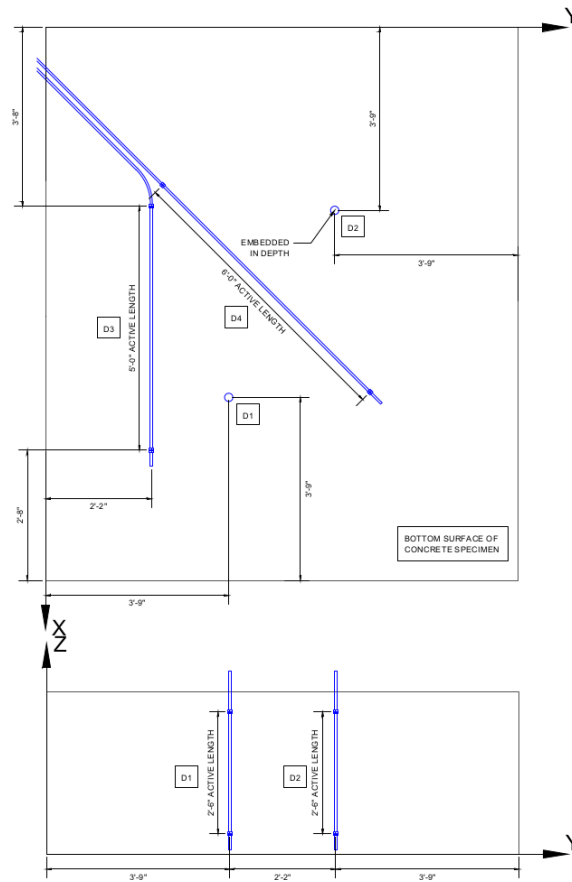


Figure 2.26: Location of deformation sensors

model outputs:

1. Vertical displacements at D1
2. Concrete strain at S1, S2, S3, S4 and S5.
3. Reinforcement strains at R1 and R2

Results to be tabulated in the accompanying spreadsheet.

## 2.3.5 P11: AAR Expansion of Nuclear Containment Vessel Followed by Earthquake

### 2.3.5.1 Description

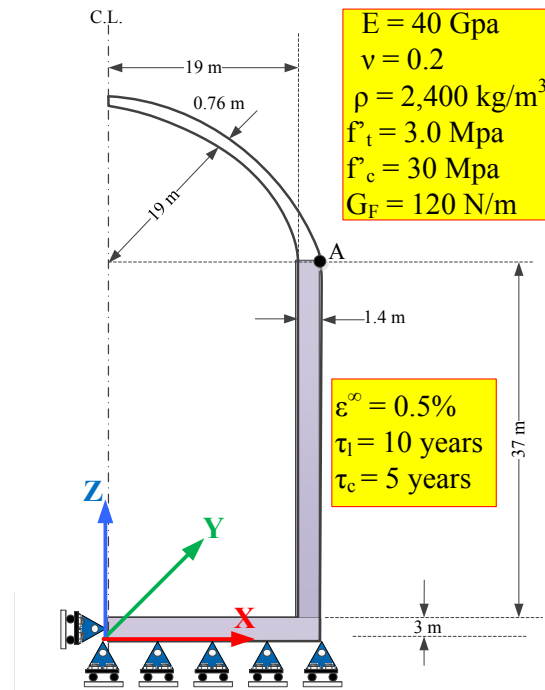
Ultimately, codes should be able to analyze nuclear containment vessel structures suffering from AAR under dynamic excitation.

Accordingly, a much simplified geometry, inspired by NUREG/CR-6706 ( (2001)), is adopted. Fig. 2.27(a) shows the dimensions as well as the key material parameters. Note that the mat foundation and the walls only are subjected to AAR, the dome is not.

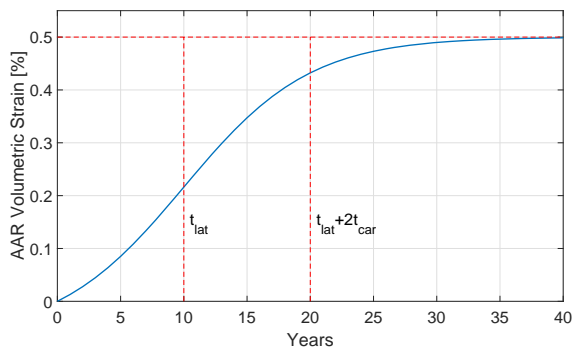
Total reinforcement is 1% vertically, and 0.5% circumferentially. Reinforcement in each direction is to be split in two layers, each 10 cm from the wall. Ignore reinforcement of the dome, however triple the elastic modulus of the concrete. Steel elastic modulus is 200 GPa, and yield stress 250 MPa.

For added clarity, the boundary conditions, and the expansion curve is shown in Fig. 2.27(b). Only gravity and AAR loads are first considered. Note that the AAR expansion is assumed to follow Larive’s curve (Larive, 1998)

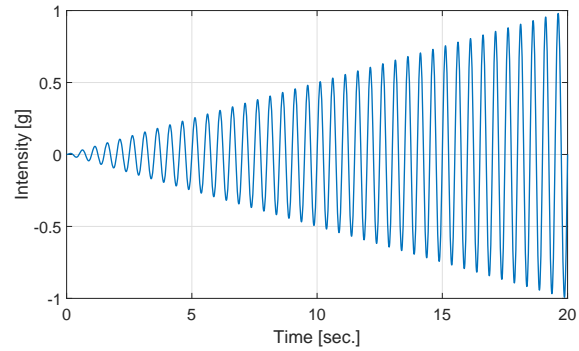
$$\varepsilon(t) = \varepsilon^\infty \frac{1 - \exp(-\frac{t}{\tau_c})}{1 + \exp(-\frac{(t-\tau_l)}{\tau_c})} \tag{2.5}$$



(a) Geometry and Material Properties



(b) Expansion Curve



(c) Expansion Curve

Figure 2.27: Characteristics of the NCVS

### 2.3.5.2 Prediction

Two sets of analyses are required:

### 2.3.5.2.1 Static

Though an axisymmetric analysis is possible, it is highly recommended that a 3D one (using 180° segment) be performed. Plot

1. Horizontal displacement of point A ( $\Delta_x$ ) versus time (increments of one month).
2. Maximum (positive) principal stress ( $\sigma_{(1)}$ ) in the wall versus time.
3. Crack profiles at  $t = [5, 10, 20, 30]$  years

### 2.3.5.2.2 Dynamic

Perform a 3D dynamic analysis, for a harmonic intensifying dynamic excitation, shown in Fig. 2.27(c), assumed to occur at age  $t = 20$  years. Assume a 5% Rayleigh damping. Report

1. Time of failure (may be defined when the analysis failed to converge).
2. Time displacement curves for point A starting with the AAR displacement that occurred at time 20 years, until failure (as defined by the user) occurs.
3. Maximum (positive) principal stress ( $\sigma_{(1)}$ ) in the wall versus time.
4. Deformed shapes and crack profiles at 1 sec. increment (starting with  $t = 0$ ) until reported failure.

Results to be tabulated in the accompanying spreadsheet.

# 3— Results Submission and Workshop

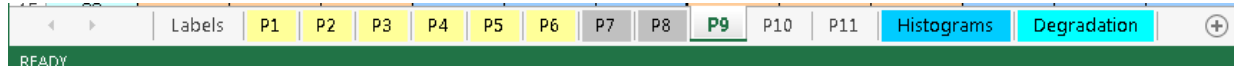
## 3.1 Excel file for Results

All results should be entered in the accompanying spreadsheet, Fig. 3.1. Note that the spreadsheet contains all available experimental data to facilitate fits, and participants must enter their prediction within the predefined cells and for the specified time increments. All cells are protected except those which can be overwritten by participant data.

This will greatly facilitate comparison of results, as a separate Matlab program could extract results from all submissions and results compared.

## 3.2 Workshop

A RILEM workshop will be held in conjunction with the annual 2018 RILEM TC-259 committee to discuss results.



(a) One tab for each Problem

	Names	Affiliation	email	Country
1				
2				
3				
<b>Computer Programs</b>				
1				
2				

Comments	

(b) Identification

Test Case P10; Idealized Dam Model												
Fixed T, RH, Load							Transient T, RH, Load					
Time	Displacement (mm)			Resultant Force MN			Displacement (mm)			Resultant Force MN		
Months	x	y	z	x	y	z	x	y	z	x	y	z
0												
3												
6												
9												

(c) Example of input cells

Static AAR			Nuclear Containment Vessel			
years	$\Delta A_c$ (mm)	$\sigma_{ci}$ (Mpa)	Dynamic (after AAR)			Failure at time:
0.00			time [sec.]	$\Delta A_c$ (mm)	$\sigma_{ci}$ (Mpa)	
0.50			0.00			
1.00			0.01			
1.50			0.02			
2.00			0.03			
2.50			0.04			
3.00			0.05			
3.50			0.06			
4.00			0.07			
4.50			0.08			
5.00			0.09			
5.50			0.10			
6.00			0.11			
6.50			0.12			
7.00			0.13			
7.50			0.14			
8.00			0.15			
8.50			0.16			
9.00			0.17			
9.50			0.18			
10.00			0.19			
10.50			0.20			
11.00			0.21			
11.50			0.22			
			0.23			

Insert Crack profile t=5 years

Insert Crack profile t=1 sec.

(d) Data input and figures

Temperature Data			
Tmax	25	A	12.5
Tmin	0	Xi	16
Tmean	12.5		

RH Data			
RH max	95	A	17.5
RH min	60	Xi	16
RH mean	77.5		

Pool Data			
EL max	95	A	17.5
EL min	60	Xi	0
EL mean	77.5		

Weeks	Temp.	RH	Stress	EL
0	0.8	61.1	-5	77.5
1	0.4	60.5	-5	79.6
2	0.1	60.1	-5	81.7
3	0.0	60.0	-5	83.7
4	0.1	60.1	-5	85.6
5	0.4	60.5	-5	87.4
6	0.8	61.1	-5	89.1
7	1.4	62.0	-5	90.6
8	2.2	63.1	-5	91.9
9	3.1	64.4	-5	93.0
10	4.2	65.9	-5	93.9
11	5.4	67.6	-5	94.5
12	6.7	69.4	-5	94.9
13	8.1	71.3	-5	95.0
14	9.5	73.3	-5	94.9
15	11.0	75.4	-5	94.5
16	12.5	77.5	-10	93.9
17	14.0	79.6	-10	93.0
18	15.5	81.7	-10	91.9
19	16.9	83.7	-10	90.6
20	18.3	85.6	-10	89.1
21	19.6	87.4	-10	87.4

(e) Example of provided input data

Figure 3.1: Sample of Excel based presentation of results

# Bibliography

- Capra, B. and A. Sellier (2003). “Orthotropic modeling of Alkali-Aggregate Reaction in Concrete Structures: Numerical Simulations”. In: *Mechanics of Materials* 35, pp. 817–830.
- Charlwood, R. G. et al. (1992). “A Review of Alkali Aggregate Reactions in Hydroelectric Plants and Dams”. In: *Proceedings of the International Conference of Alkali-Aggregate Reactions in Hydroelectric Plants and Dams*. Ed. by CEA and CANCEL. Fredericton, Canada, pp. 1–29.
- Divet, L. et al. (2003). *Aide à la gestion des ouvrages atteints de réactions de gonflement interne: Guide méthodologique*. Tech. rep. Laboratoire Central des Ponts et Chaussées (LCPC).
- Gilks, P. and D. Curtis (2003). “Dealing with the Effects of AAR on the Water Retaining Structures at Mactaquac GS”. In: *Proceedings of the 21st Congress on Large Dams*. Montreal, Canada, pp. 681–703.
- Institution of Structural Engineers (1992). *Structural effects of alkali-silica reaction. Technical guidance on the appraisal of existing structures*. Tech. rep. Report of an ISE task group.
- Larive, C. (1998). “*Apports Combinés de l’Experimentation et de la Modélisation à la Compréhension del’Alcali-Réaction et de ses Effets Mécaniques*”. PhD thesis. Paris: *Laboratoire Central des Ponts et Chaussées*.
- Léger, P., P. Côte, and R. Tinawi (1996). “Finite Element Analysis of Concrete Swelling Due to Alkali-Aggregate Reactions in Dams”. In: *Computers & Structures* 60(4), pp. 601–611.
- Multon, S. and F. Toutlemonde (2006). “Effect of Applied Stresses on Alkali-Silica Reaction Induced Expansions”. In: *Cement and Concrete Research* 36(5), pp. 912–920.
- NUREG/CR-6706 (2001). *NUREG/CR-6706: Capacity of Steel and Concrete Containment Vessels With Corrosion Damage*. <http://pbadupws.nrc.gov/docs/ML0110/ML011070123.pdf>.
- Poole, A.B. (1992). “Introduction to Alkali-Aggregate Reaction in Concrete”. In: *The Alkali-silica Reaction in Concrete*. Ed. by R.N. Swamy. Van Nostrand Reinhold, New York, pp. 1–28.
- Saouma, V. and L. Perotti (2006). “Constitutive Model for Alkali Aggregate Reactions”. In: *ACI Materials Journal* 103(3), pp. 194–202.
- Sellier, A. et al. (2009). “Combination of structural monitoring and laboratory tests for assessment of alkali aggregate reaction swelling: application to gate structure dam”. In: *ACI Material Journal*, pp. 281–290.